Martensitic Phase Transitions

Winfried Petry and Jürgen Neuhaus
Physik Department E13, Technische Universität München,
D-85748 Garching, Germany

Many elements transform from a high temperature bcc phase to a more dense packed low temperature phase. The great majority of these transitions are of 1st order, displacive and reconstructive. The lattice potentials which govern these martensitic transitions can be probed by inelastic neutron scattering, thereby answering fundamental questions like: Will the transition be announced by dynamical or static lattice fluctuations? What are the trajectories for the displacements needed for the transformation? Does the vibrational entropy stabilize the high temperature phase? Are the unusual transport properties in theses materials related to their ability to transform?

1 INTRODUCTION

Almost half of the elements condense in the open bcc structure. With very few exceptions these bcc phases transform into a close packed structure at lower temperature or under pressure [1]. Among the exceptions those with magnetic transitions will be noted: Pure iron solidifies at 1809 K in the bcc δ-phase and undergoes a first transition to fcc γ-Fe at 1665 K. Very unusual it transforms with decreasing temperature back to a bcc α-phase at 1184 K. Within this α-phase a magnetic transition occurs at 1042 K below of which α-Fe is ferromagnetic. Pure cobalt solidifies immediately in a closed packed fcc structure and has its ferromagnetic transition within this β-phase at 1388 K. On further cooling it transforms to hcp α-Co at 693 K without any apparent influence on its magnetic properties.

In all cases the transitions are *displacive* and of *first order*. They are mostly *reconstructive* in the sense that the high temperature/low pressure or parent phase and the product phase are not related by a group-sub group relation. Rather, the product phase reconstructs a new structure belonging to a different symmetry group. This reconstruction is achieved by homogenous lattice distortive strains and/or by shuffles. A lattice distortive strain is a homogenous strain that transforms one lattice into another. A shuffle is a coordinated movement of atoms that produces in itself no lattice distortive deformations but alters the symmetry of the crystal. A shuffle deformation can be expressed by a lattice wave modulation of a short wavelength, typically in the order of one to a few nearest neighbour distances. The lattice correspondence observed between parent and product phase defines a structural unit in the parent phase that under the action of homogeneous strain and/or shuffle transforms into a unit of the product phase. Discerning this lattice correspondence does not mean that the actual trajectory for the displacive deformation is known, many ways through real space produce identical lattice correspondences.

Firstly, the question will be adressed *whether the actual trajectory for the displacements during the transition can be deduced from the dynamical response of the lattice.* In harmonic approximation the phonon frequencies $\omega(\vec{q})$ are given by the eigenequation

$$\omega^2(\vec{q})\cdot\vec{e}(\vec{q}) = \overline{\overline{D}}(\vec{q})\cdot\vec{e}(\vec{q}) \tag{1}$$

with $\vec{q}$ the phonon wave vector and $\vec{e}(\vec{q})$ the eigen- or polarizationvector. In high symmetry directions the latter describe longitudinal and transversal displacements. For monoatomic systems the components of the dynamical matrix $\overline{\overline{D}}(\vec{q})$

$$D_{\alpha\beta}(\vec{q}) = {}^{1}\!/_{M}\sum_{mn}\phi_{\alpha\beta}^{mn}\cdot\exp\{i\vec{q}\,\vec{r}^{m}-\vec{r}^{n}\} \tag{2}$$

can be expressed in terms of the Fourier transform of the force constants ϕ which are the second order derivatives of the interatomic potentials. For convenience the summation in eq (2) restricts to a small number of nearest neighbour shells. Translational symmetry of the lattice implies that the possible solutions for the eigenfrequencies $\omega(\vec{q})$ can be projected into one reciprocal unit cell. In the limit of long wave length $\vec{q}\rightarrow 0$, i.e. when the lattice is seen by the phonon as a continuum $\omega(\vec{q})$ depends linearily on q.

$$\omega^2(\vec{q})\cdot\rho = C_{ij}(\vec{q})\cdot q^2 \tag{3}$$

Here ρ means the mass density and cubic symmetry reduces the elastic constants C_{ij} to a bulk modulus $K = 1/3(C_{11} + 2C_{12})$ expressing the static compressibility $\chi = 1/K$ and the two independent shear moduli C_{44} and $C' = \frac{1}{2}(C_{11} - C_{12})$. Eq. (1-3) indicate how lattice vibrations probe the lattice potential in 3 dimensions.

It is expected that the transition occurs in such a direction where low energy phonons or particularly low elastic constants indicate a weak repulsive interaction for displacements. *Where in reciprocal space shall we find the low energy phonons? At very short momentum transfer $\vec{q}$ or at large $\vec{q}$ close to the Brillouin zone boundaries?* Answering these questions will tell us whether long wavelength shears or short wavelength shuffles dominate the transformation. Following this idea we expect dynamical precursors for a transition of first order. Eventually these dynamical anomalies become stronger the closer the temperature approaches the transition. These dynamical precursors are the fingerprint of the approaching transition, but we will learn that at the same time they are the cause for stabilizing the open bcc structure. *It is interesting to speculate whether these large amplitude phonons freeze to static displacements and thereby cause elastic precursors.* Discussion on this question deeply involves the role of defects and nucleation for the transition. The great resemblance of elastic and inelastic diffuse scattering will give us an intuitive picture of the liquid-like motions of rows of atoms along the nearest neighbour direction. Finally we show how the tendency of these elements to transform into close packed structures dominates other physical properties: *anomalies in the transport mechanism, strongly anharmonic lattice potentials* etc.

Most of this holds for transitions from bcc → close packed structures. *But what happens if the reverse transition occurs? - or a transiton within close packed structures like fcc → hcp?* Observing the dynamical response of iron and cobalt will partly answer this questions.

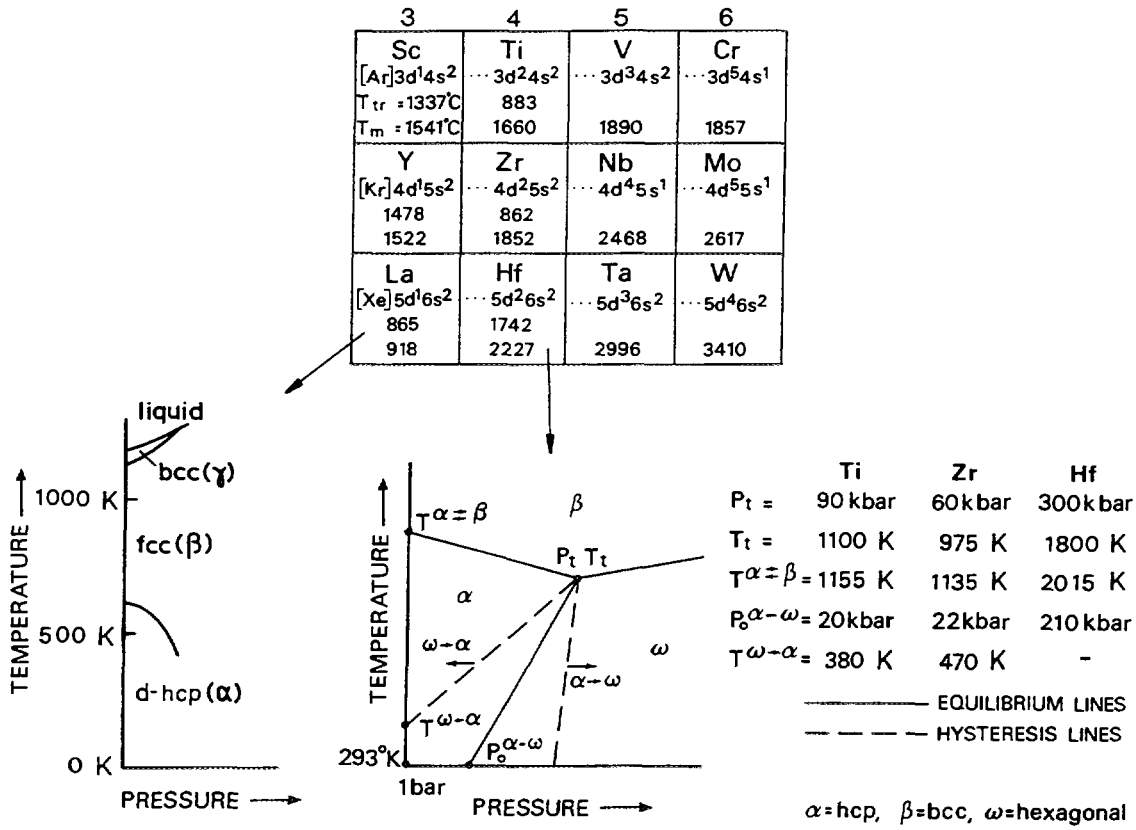

Fig. 1: Transition temperatures T_0 and phase diagramms for the early transition elements.

Metallurgists and physicists do not agree on a unique definition of what is meant by a martensitic phase transition. Originally the term was introduced for the segregation of a bct phase within γ or austenitic steel during cooling down in honour of the German metallurgist A.Martens. Soon the expression was extended to all kinds of displacive transitions. Throughout this paper martensitic transitions are discussed in a more physical sense: i) The transition occurs instantaneously, and is virtually independent of time. ii) The amount of transformation is a characteristic of the temperature, i.e. a hysteresis exits. iii) The transformation is very reversible. In general the same single crystal is obtained after a temperature cycle. In reality this is difficult to achieve due to experimental constrains. iv) Insofar as alloys are concerned, no change occurs in the chemical composition and almost no change in volume is observed. v) There exists a definite orientational relation between the parent and product phase. In general a habitus plane is common to parent and product phase. vi) No group-subgroup relation exists between the two structures. The product phase reconstructs its own group symmety. For the above reasons martensitic transitons are of 1st order, they are displacive and reconstructive. The latter makes them different from a whole class of 2nd order transitions like the ferroelectric transition in $SrTiO_4$. For a recent review of some of the principles we refer to [2].

Martensitic transformations are mainly studied in binary or tertiary alloys, particularly if the shape memory effect is of primary interest. However, if the basic physical properties are addressed, it is extremely helpful to return to elementary systems. In general the structural properties of monoatomic solids are better defined. The influence of all kinds of defects can be thoroughly controlled and phenomena induced by host-defect interactions are expected to be of minor importance. Further, quite a number of martensitic transitions in the elementary systems occur at high temperatures, i.e. thermal equilibrium during the transition is easily achieved. The inherent drawback is the difficult experimental access to single crystals in the high temperature phase – this is also the reason why experimental information on high temperature martensitic transitions is scarcely available. Indeed recent progress in studying high temperature martensitic transitions is due to the development of reliable in-situ growth methods of parent phase single crystals during the experiment [3].

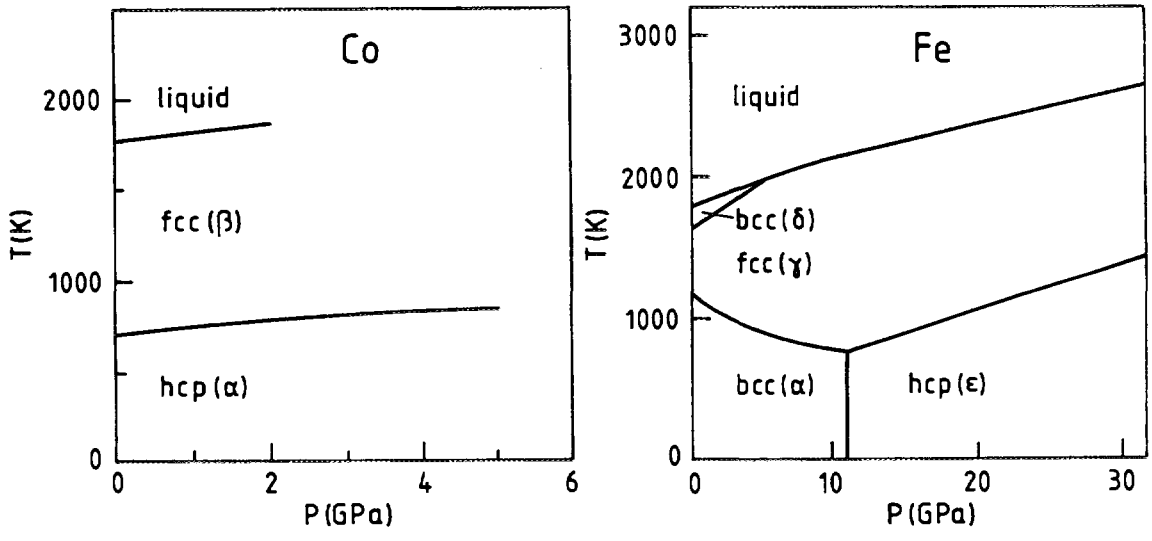

Fig. 2: Phase diagramms for iron and cobalt.

Being interested in dynamical properties of the transition, the choice of experimental methods is almost limited to inelastic neutron scattering. Whereas elastic constants are conventionally measured by ultrasonic methods, this is no longer feasable for the high temperature phases. Further, elastic constants contain only direct information about long wavelength shears. Dynamical instabilities towards opposite shuffles of neighbouring planes have to be explored in full reciprocal and energy space which is only accessible through inelastic neutron scattering.

2 TRANSITIONS FROM BCC → CLOSE PACKED STRUCTURES

Prominent examples for transitions from the open bcc structure to closest packed structures are the alkali, earth alkali and the group 3 and 4 transition elements. Transitions in Li or Na to 9R+fcc and 9R+hcp occur at 75 K and 35 K, respectively. These were amoung the earliest elementary systems in which one was looking for dynamical precursors of the martensitic phase transition. Despite a considerable effort by neutron scattering experiments [4,5] the outcome was to a certain extent disappointing: Dynamical precursors close to the transition temperature are virtually absent. Elastic precursors have been observed but their strength and location in $\vec{q}$-space often depend on

the thermal history of the crystal. Recent ab initio [6] and thermodynamic [7] calculations describe some of the reasons: Energetically the different closest packed structures are hardly separable and the actual product phase is strongly influenced by the initial crystal quality and thermal history.

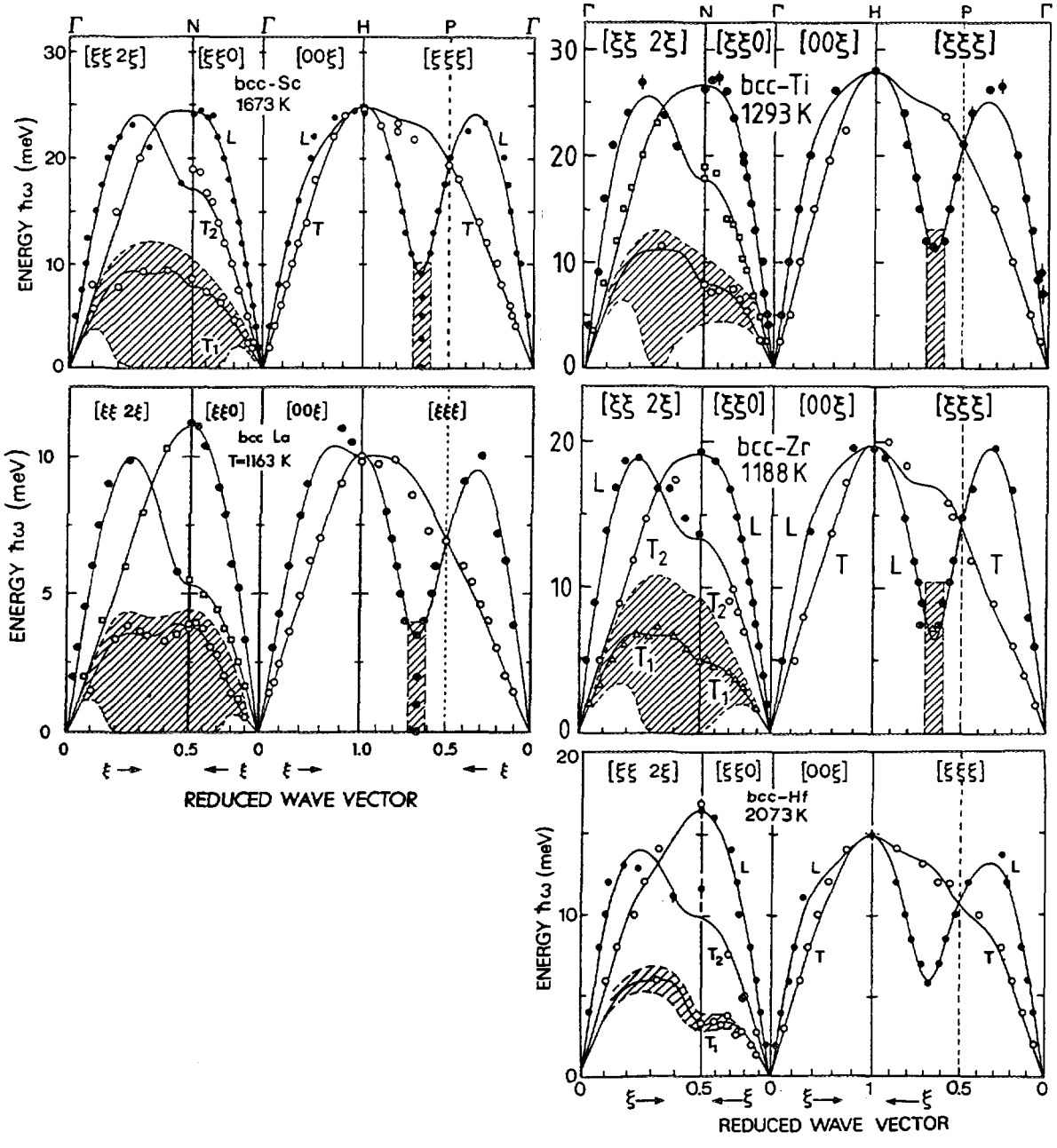

Fig. 3: Measured phonon dispersions in the bcc phase of group 3 and 4 metals. Shaded areas indicate regions of inelastic diffuse scattering or strongly damped phonons. [10-14]

The situation is very different in the early transition metals. As indicated in Fig. 1, Sc, Y, La, Ti, Zr and Hf all transform into the hcp structure. For the group 4 elements an additional transition to the ω-phase under moderate pressure is known. As an exception, La first transforms to fcc and then to double-hcp. Stassis and collaborators [8] were the

first to measure the phonon dispersion of β-Zr by cycling a large α-single grain through the α-β transition. More detailed measurements could be made by the in-situ growth technique developed more recently [9]. Fig. 3 gives a synopsis of the measured phonon dispersions in the parent bcc phase of these elements [10-14].

The dispersions in Fig. 3 greatly resemble one another, i.e. the phonons at higher energy scale roughly with the square root of the mass and the lattice constant, thereby following the homology rule. Most evidently all dispersions are dominated by a few unusual properties: i) At $\xi = 2/3$ the longitudinal L[ξξξ] phonon branch shows a pronounced dip. ii) The whole transverse $T_1[\xi\xi 0]$ phonon branch with $[1\bar{1}0]$ polarisation is of low frequency when compared to other transverse phonons. iii) The same holds true for the off symmetry $T_1[\xi\xi\ 2\xi]$ phonon branch. iv) The low energy phonons are strongly damped. As indicated by the shaded area the intensity of these damped phonons reaches down to zero energy transfer.

2.1 The bcc → ω transition

The atomic displacements achieved by a longitudinal phonon in [ξξξ] direction with $\xi = 2/3$ have a particular crystallographic meaning for the bcc structure. As shown in Fig. 4, for a stationary wave at $\xi = 2/3$ two of three neighbouring (111) planes move towards each other, whereas every third plane stays at rest. When the two moving planes collapse the perfect ω structure is achieved. During the second half of the wave, the planes move in the opposite direction and approach the plane at rest. Distortions in these directions are called anti-ω distortions. From symmetry, it is evident that the restoring forces involved for distortions into the ω or anti-ω structure are different.

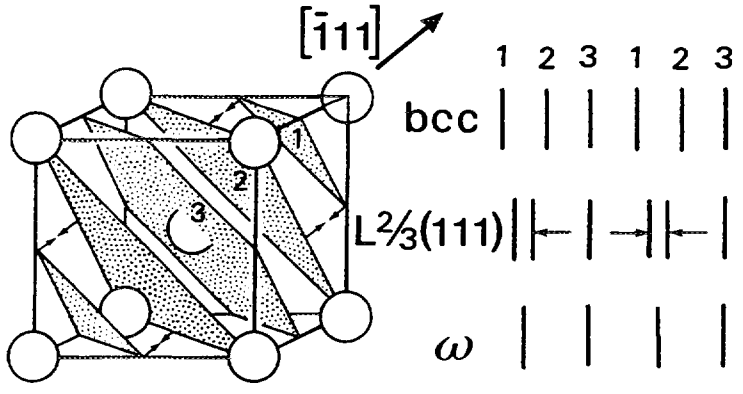

Fig. 4: Scheme of the bcc→ω transition.

The ω lattice can be described as an hexagonal cell, with the *c* axis along the $\langle 111\rangle_{bcc}$ direction and the *a* axis along the $\langle 110\rangle_{bcc}$ direction. Thus the crystallographic relation between ω and β reads

$$(111)_{bcc} \,||\, (00.1)_{\omega} \text{ and } [\bar{1}01]_{bcc} \,||\, [01.0]_{\omega}$$

Fig. 5 illustrates what is meant by the shaded area in Fig. 3 at L2/3(111). *Coherent* intensity is measured down to zero (!) energy transfer and even has its maximum at zero energy. Further, the small elastic peak on top of the broad inelastic scattering distribution

is of purely incoherent origin and therefore does not represent any coherent elastic scattering. The latter is of particular importance because any static embryo of the ω-phase causes elastic diffuse scattering at $\bar{Q}$ = 4/3(111), i.e. at the scattering vector $\bar{Q}$ where the spectra in Fig. 5 have been measured. Therefore the absence of this "truly" elastic scattering means that within the time window of the method ($\leq 10^{-10}$s) no stable ω-embryo exists.

Taking resolution effects into account, the broad inelastic distribution can be reproduced by a damped oscillator, the scattering law of which reads

$$S(Q,\omega) = f(Q)\frac{1}{1-e^{-\hbar\omega/k_BT}}\cdot\frac{\Gamma\hbar\omega}{\left(\hbar^2\left(\omega^2-\omega_0^2\right)\right)^2+(\Gamma\hbar\omega)^2} \qquad (4)$$

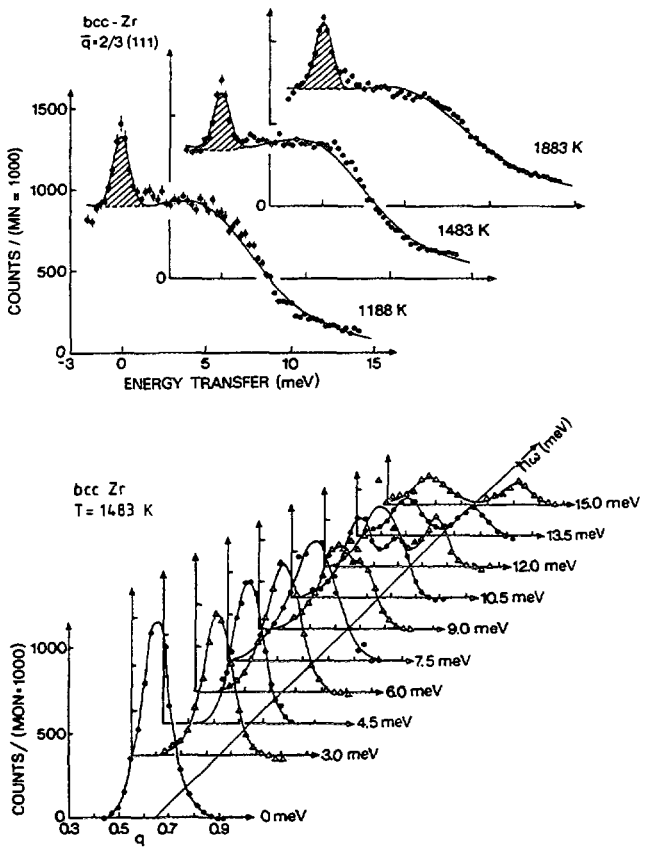

Fig. 5: The L2/3(111) phonon measured at $\bar{Q}$ = 4/3(111). Top: Const. q-scans at different temperatures. The elastic peak on top of the broad energy distribution is of purely elastic incoherent origin. Bottom: The evolution of the dispersion around $\bar{Q}$ = 4/3(111) towards a region of diffuse inelastic intensity is visualized by a series of const. E-scans. For the elastic scan the incoherent intensity has been subtracted [11].

With the exception of β-Hf, the actual damping term Γ observed for the different elements in Fig. 3 is larger than the resonance frequency ω_0 itself. This means that the L2/3(111) phonon has an extremely short lifetime, the amplitude of the corresponding displacement is over-damped after one period of the vibration. This short lifetime of the L2/3(111) excitation has to be well separated from the question of how this phonon

propagates in real space. Along L[ξξξ] direction a strong dispersion is observed whereas in the vicinity of $\bar{Q}$ = 4/3(111) and in directions perpendicular to [ξξξ], i.e. in T$\left[\xi\xi\,\overline{2\xi}\right]$ and T$\left[\xi\bar{\xi}0\right]$ only a very weak dispersion is observed. Translated to real space this means that the displacements corresponding to the L2/3(111) phonon propagate along the [111] chains but neighbouring [111] chains mostly do not follow. Considering both, the short lifetime and the localized character of this phonon, propagation perpendicular to [111] is *liquid-like*.

In the single-oscillator approximation, the amplitude u_0 of a vibration is given by

$$u_0 = \left(\frac{2k_BT}{m}\right)^{1/2} \cdot \frac{1}{\omega_0} \qquad (5)$$

The phonon energies at L2/3(111) are in the order of 3-10 meV corresponding to displacements from 0.4-0.75 Å at the transition temperature T_0. These values are comparable to the displacemenets needed for the bcc → ω transition. Whereas these large displacements are certainly indicative for the weakness of the bcc lattice towards the ω transformation their absolute values have to be taken with caution, eq. (5) is only a crude approximation, and inserting the mass of a single atom is probably not justified.

As depicted in Fig. 6 the open bcc structure is characterized by chains of nearest-neighbour (NN) atoms in [111] directions. Out of all phonons in the L[ξξξ] branch, the phonon at ξ = 2/3, i.e. λ = $\sqrt{3}/3\,a$, is the only one which leaves the [111] chains undisturbed. Thus atoms along [111] , i.e. the direction with shortest distances between the atoms and therefore strong restoring forces, do not alter their distance. The phonon frequency is low because it is determined by restoring forces between the chains which are weaker (because they do not compress the NN chains). All the other modes with [111] propagation will change the distances of the atoms along the chains, thus giving rise to extra restoring forces leading to higher energies.

This purely geometrical argument is valid for *all* bcc structures and therefore cannot explain the difference in softening of the L2/3(111) phonon in different transition elements. Whether this general weakness of the bcc lattice towards the ω-structure is enhanced or not depends on the filling of the d-electrons. Ab initio calculations by Ho et al [15] show that in bcc Zr the valence charge density is concentrated in d bonds which run in chains along (111) direction with very little interaction between neighbouring chains, i.e. the valence charge is highly localized along these [111] chains. As mentioned before, the L2/3(111) phonon is the only one which leaves the [111] chains undisturbed, and does not compress or stretch the highly localized d bonds. The validity of these considerations is underlined by results from similar calculations for bcc Mo [15]. Here the d bonds entangle the [111] chains. Therefore the L2/3(111) phonon is not expected to have a particularly low frequency, perfectly agreeing with the experimentally determined phonon dispersion of Mo. Fig. 7 shows the valence charge distribution in the (110) plane for bcc Zr and Mo, respectively. To visualize the effect of these charge distributions on the restoring forces, the densities in Fig. 7 are force weighted, i.e. shown for small displacements. Chromium which is chemically equivalent to Mo may serve as an example of a phonon dispersion for a bcc element exhibiting almost no dip at L2/3(111) -

see Fig. 8. The electronic calculations as presented in Fig. 7 are ground state calculations. How important finite temperature can be is also shown in Fig. 8. The dispersion of Cr at 1773 K has changed considerably and very much resembles of that of the group 3 and 4 transition metals.

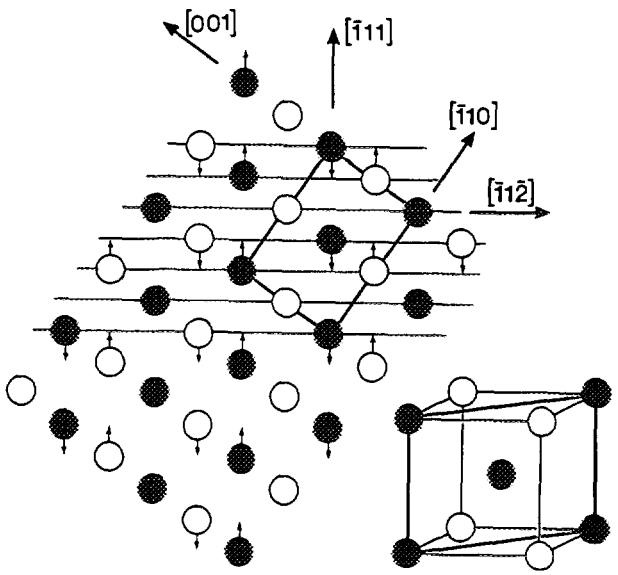

Fig. 6: Displacements of the atoms in a (110) plane due to a L2/3(111) phonon.

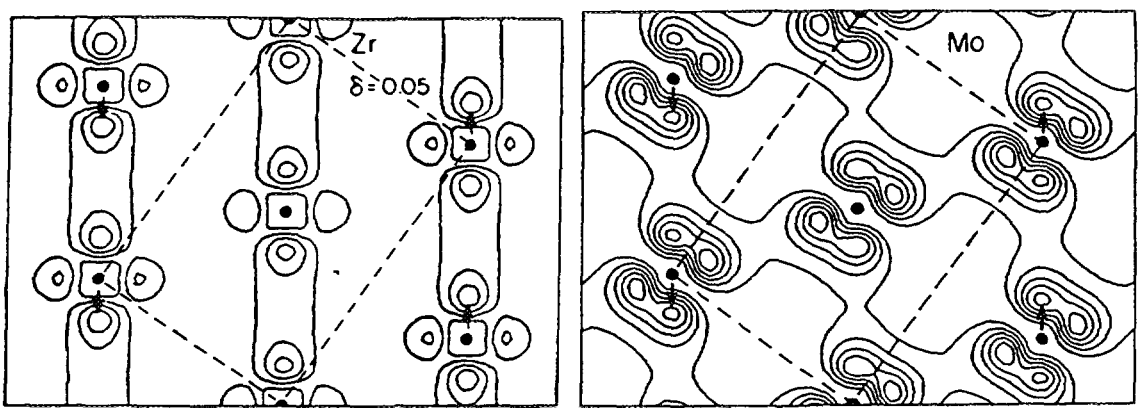

Fig. 7: Contour plots of the valence charge density in the bcc (110) plane. Densities are force weighted [15,16].

Returning to our initial interest that of the bcc → ω transition, we summarise the experimental observations: i) The high temperature bcc phases show large amplitude fluctuations towards the ω structure. These excitations do not alter with temperature and are also observed in bcc metals of group 3 which do not transfer to the ω phase. The low restoring force for the shear motion of the [111] chains towards each other is therefore a property inherent to the open bcc structure. For a more fundamental ab-initio explanantion on the basis of the electronic configuration, we refer to literature [15]. ii) The L2/3(111) shuffle alone transforms the bcc lattice to a ω lattice. There is no need for any long wavelength shear. iii) In pure metals no static precursors of the parent phase are observed. As only dynamical precursors exist, the description of a homogenous transition is more appropriate.

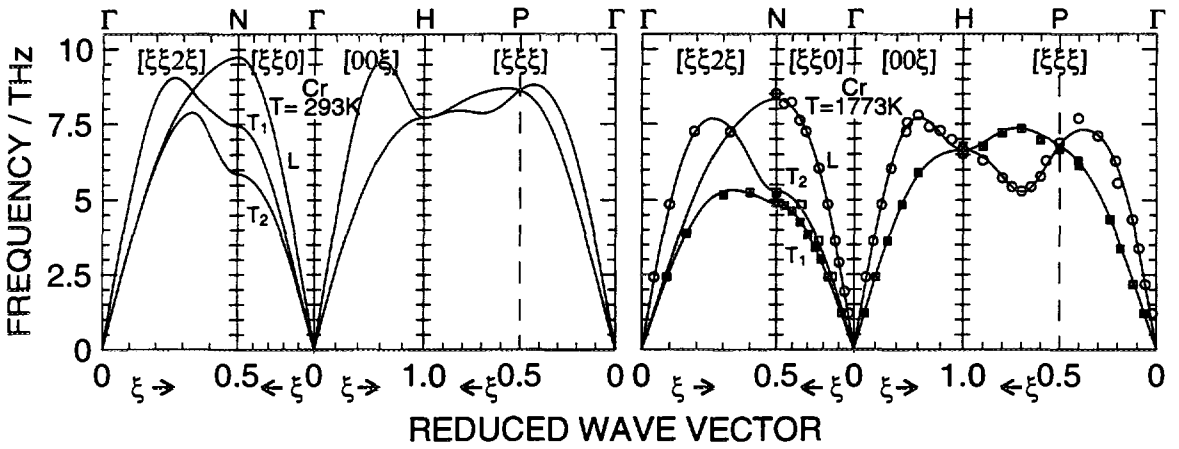

Fig. 8: Dispersion of Cr measured at RT[16] and 1773 K[17]

2.2 The bcc → hcp transition

The crystallographic relation for the bcc → hcp transition has been established by Burgers [18].

$$(110)_{bcc} \,||\, (00.1)_{hcp} \text{ and } [\bar{1}\,11]_{bcc} \,||\, [\bar{2}\,1.0]_{hcp}$$

The transformation can be achieved by the combined displacements of two phonons. The transverse zone boundary phonon $T_1 1/2(110)$ at the N point with a displacement of neighbouring (110) planes in opposite $[1\bar{1}0]$ directions by $\delta = a \cdot \sqrt{2}/12$ achieves the hcp stacking sequence. Two equivalent long wavelength shears – for instance $(1\bar{1}2)[\bar{1}\,11]$ and $(\bar{1}\,12)[1\bar{1}\,1]$ – squeeze the bcc octahedron to a regular hcp one, thereby changing the angle from 109.5° to 120°. This Burgers mechanism is illustrated in Fig. 9.

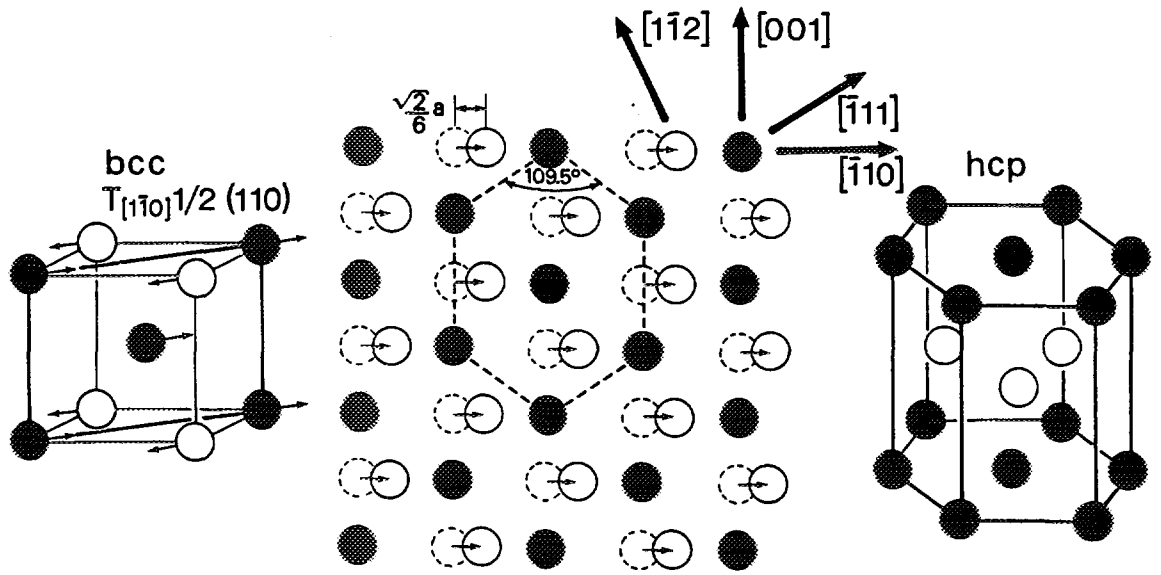

Fig. 9: Scheme of the bcc → hcp transition (Burgers mechanism).

The $T_1 1/2(110)$ phonons in Fig. 3 are of even lower energies than the so-called ω phonons, i.e. the bcc lattice exhibits very low restoring forces for shuffling neighbouring (110) planes into opposite $[1\bar{1}0]$ directions. As for the ω point these phonons are strongly damped. Contrary to what has been observed at the ω point, the $T_1 1/2(110)$ phonon energy considerably decreases on approaching the martensitic transition temperature - see Fig. 10. Because the bcc $\rightarrow$ ω transition is driven by an increase in the pressure, the temperature variation does not alter the related L2/3(111) phonon. The bcc $\rightarrow$ hcp transition however, is driven by temperature and therefore the related $T_1 1/2(110)$ phonon decreases with decreasing temperature. Nevertheless the martensitic transition occurs at finite energy.

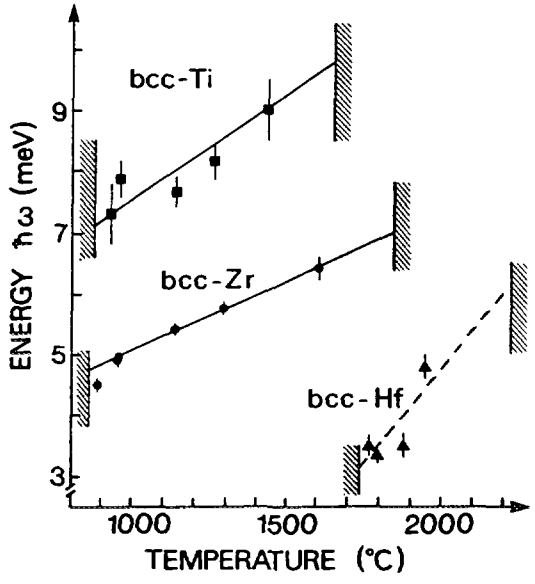

Fig. 10: Temperature dependence of the $T_1 1/2(110)$ phonon in β-Ti, β-Zr and β-Hf [21].

The shears needed to complete the transition are those given by the initial slope of the $T_1[\xi\xi\, 2\xi]$ phonon branch. The elastic constant along this direction is rather low, i.e. one finds low restoring forces for this motion. Recent thermodynamic approaches [19,20], which use an expansion of the free energy in terms of dynamical displacements have suggested that a small softening of the relevant low-energy phonon is sufficient to produce a lower minimum of the free energy required to obtain the product phase. The order parameter in the expansion of free energy is related to the *average* atomic displacements of the phonons which are associated with the transition.

The fact that the $T_1 1/2(110)$ phonon and the initial slope of the $T_1[\xi\xi\, 2\xi]$ branch are of little value do not unequivocally prove that the actual trajectory of the atoms during the transition follow the Burgers mechanism. Computations of energy landscapes may be helpful in filling this argumentative gap. For the pressure induced bcc $\rightarrow$ hcp transition in Ba Chen et al [22] calculated the valley of lowest internal energy as a function of the Burgers shuffle and the homogeneous strain needed to squeeze the octahedron - Fig . 11. As it turns out, this valley of lowest energy for the combined deformation follows exactly the trajectory assumed in the Burgers mechanism.

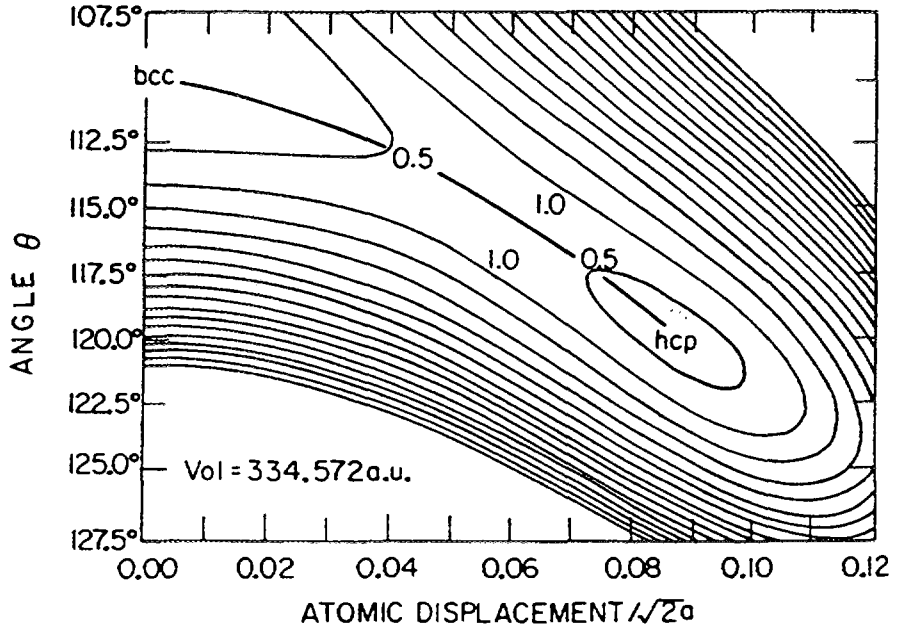

Fig. 11: Energy landscape for the bcc → hcp transition in Ba [22]. The transition is supposed to occur along the valley of lowest energy. Θ is the angle of the octahedron, displacements are along [110] as indicated in Fig. 6.

We conclude that low frequencies along the $T_1[\xi\xi 0]$ phonon branch which further decrease upon approaching T_0 are indicative for the Burgers mechanism. Different to the ω transition, the bcc → hcp transformation needs a combination of a short wavelength shuffle and a homogenous lattice strain.

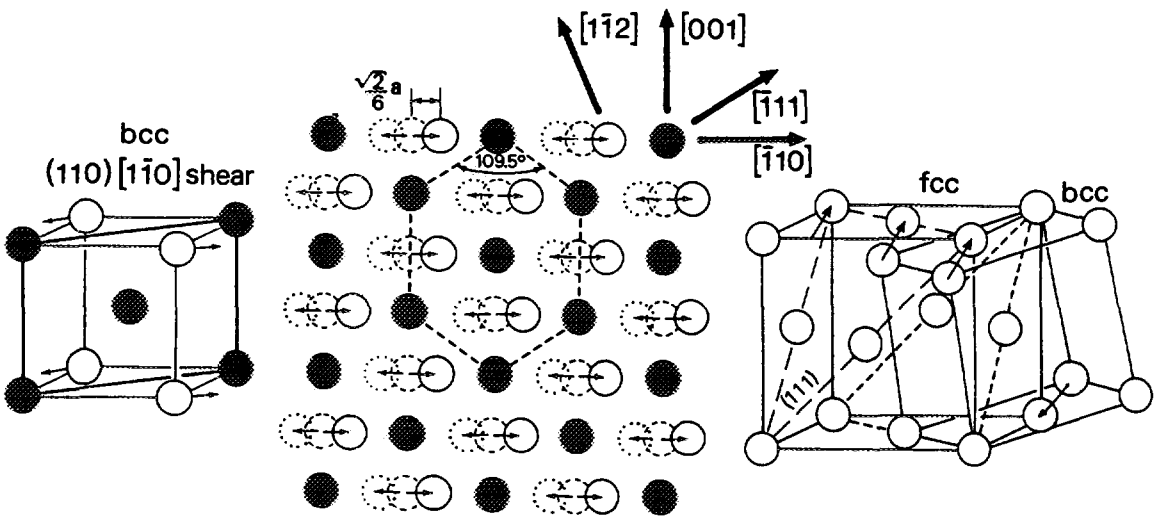

Fig. 12: Scheme of the bcc → fcc transition.

2.3 The bcc → fcc transition

Before discussing the γ → β transition in La as an example for the bcc → fcc transformation, we have to recover some arguments concerning the relation of the

phonons involved in the ω and hcp transition. The longitudinal displacements of the (111) planes for the L2/3(111) phonon can also be viewed as a shearing of neighbouring [111] rows in opposite directions [23], i.e. L2/3(111) ≡ $T_{[11\bar{1}]}$1/3(112). Noting also the identity $T_{[01\bar{1}]}$1/2(112) ≡ $T_{[1\bar{1}0]}$1/2(110) the phonons related to the two above mentioned transitions are no longer isolated points in reciprocal space but are part of the valley of the transverse low energy phonons along [ξξ2ξ] propagation.

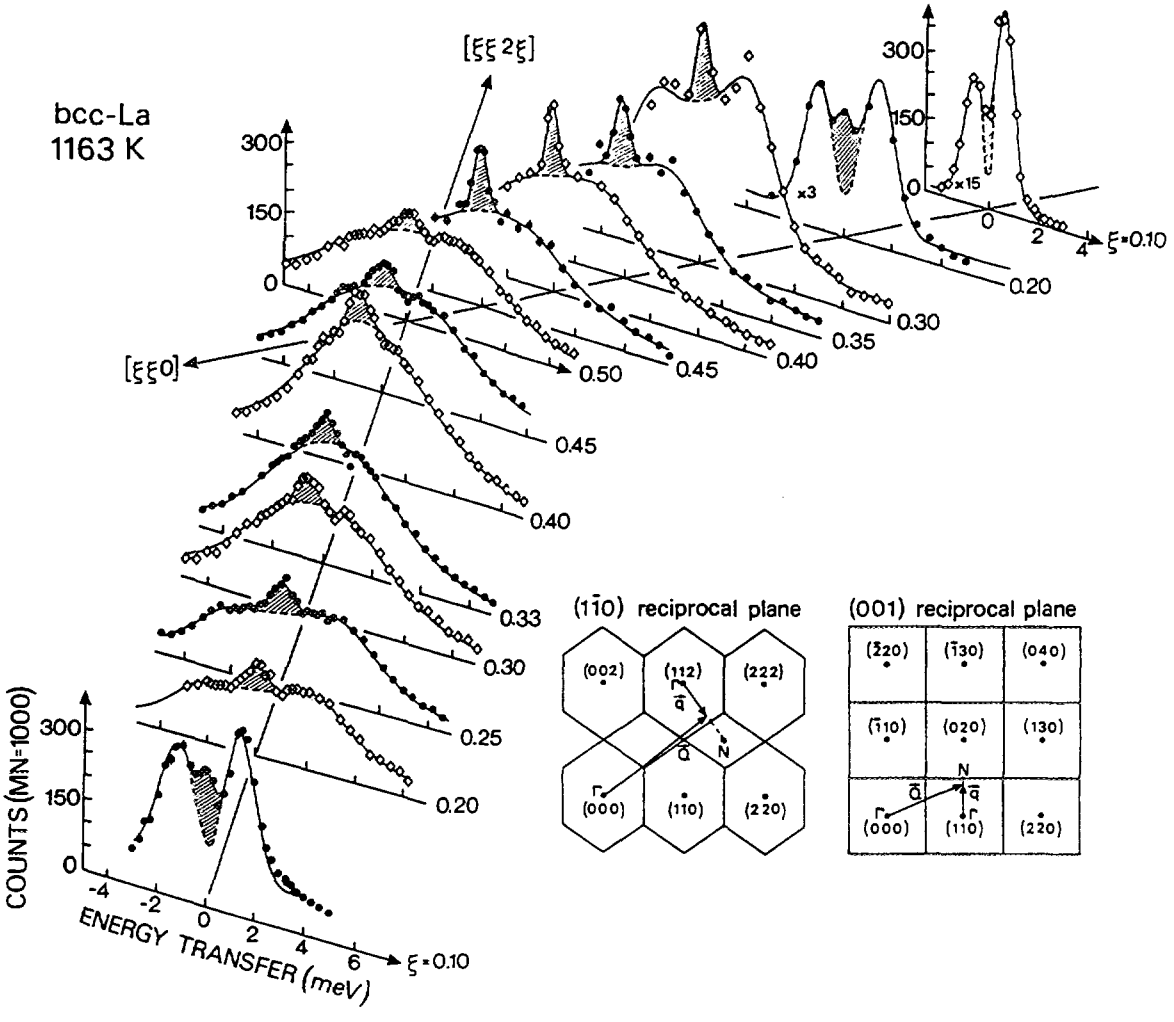

Fig. 13: Low energy and damped phonons along $T_1[\xi\xi 2\xi]$ and $T_1[\xi\xi 0]$ in γ-La [14].

Now, the dispersion of γ-La shows the same anomalies as the other high temperature bcc phases but instead of transforming to ω or hcp, it first transforms into fcc - see Fig. 1. Both fcc and hcp are closest packed structures and differ only by their stacking sequence of the basal plane. As for the bcc → hcp transition a short wavelength shuffle shifts the ABAB...sequence of $(110)_{bcc}$ planes to an ABAB... sequence of densly packed basal planes. But a further $(110)[1\bar{1}0]_{bcc}$ long wavelength shear is needed to change to the ABCABC... sequence of $(111)_{fcc}$ planes - see Fig. 12. Hence this mechanism is analogous to the Burgers mechanism, as both transitions preserve the interlayer distance of the original $(110)_{bcc}$ plane and thus the replusive effect of one layer with respect to the

other. The essential difference is that for the bcc → fcc transition a further long wavelength strain of $(110)_{bcc}$ planes into $[1\bar{1}0]$ direction is neeeded. The corresponding elastic constant $C' = 1/2(C_{11}-C_{12})$ is given by the initial shape of the $T_1[110]$ phonon branch. Indeed a very low C' is found in γ-La, which is best expressed by the unusual high assymetry parameter for the two shear constants $A = C_{44}/C' \cong 10$ [14]. Similar considerations hold for the δ → γ transition in Fe. Also in δ-Fe a large $A = 7.1$ is found [24].

The dominating role of C' is confirmed by thermodynamic considerations. Assuming no volume change through the γ → β transition, it can be shown that the local restoring forces tending to oppose the change into the fcc phase solely depend on the shear constant C', i.e. a small C' alone already indicates low potential barriers for a bcc → fcc transition.

2.4 Consequences of the martensitic transition

The dynamics of the high temperature bcc phases of the group 3 and 4 metals is dominated by a valley of phonons of unusual low energy and strong damping along [ξξ2ξ] and [ξξ0] propagation. The example demonstrating this for γ-La is depicted in Fig. 13. Along this valley in the 4 dim. $\bar{Q}$-ω space, we find all the large amplitude fluctuations one needs to transform the bcc lattice to ω, hcp, fcc or related structures like 7R, 9R, d-hcp etc... Which of these locks in at the transition can hardly be determined from the phonons themselves, it depends on subtle details of the free energy of the product phase.

2.4.1 What stabilizes bcc?

The other question as to why bcc is stable at high temperature although considerable fluctuations towards close packed structures are observed is easier to answer. Knowing the phonon dispersions in the parent and product phase, vibrational entropy changes ΔS_v at the transition temperature can be calculated rather precisely in *quasiharmonic* approximation [25].

$$S_v = -3k_B \int d\omega\, Z(\omega)\{n(\omega)\ln n(\omega) - [1+n(\omega)]\ln[1+n(\omega)]\} \qquad (6)$$

$$\Delta S_v = S_{v,aboveT_0} - S_{v,belowT_0}$$

where $n(\omega) = \left(\exp\{\hbar\omega/k_BT\}-1\right)^{-1}$. A comparison with the known excess enthalpy $\Delta S_{tot}\cdot T_M$ of the bcc → close packed transition –see Table 1 – shows that roughly 2/3 of the excess enthalpy is due to the vibrational entropy. The latter is dominated by the low-energy phonons. The remaining ΔS_{tot} - ΔS_v = ΔS_{el} can then be ascribed to the difference in electronic entropy ΔS_{el}. For the particular case of δ-Fe [24] the change in vibrational entropy is even larger than the total entropy change, i.e. electronic contributions destabilize the bcc high temperature phase in Fe. Consequently, the role of these transverse energy phonons is two fold: *they are due to the instability of the bcc lattice towards a martensitic transition but in the same instance bcc is stabilized due to their contribution to the vibrational entropy.*

These considerations are not limited to the elementary systems. Ultrasonic and neutron measurements on a series of Cu based tertiary shape memory alloys [23,26] show

similar low energy phonons as in the group 3 and 4 metals. In particular large anisotropy parameters A are found. Hence it can be concluded that in the Cu based alloys also, the martensitic transformation is practically a pure vibrational driven transition [26].

Table 1: Vibrational ΔS_v and total entropy changes ΔS_{tot} at the bcc → close packed transition

	T_0(K)	ΔS_v (k_B/atom)	ΔS_{tot} (k_B/atom)
Ti	1156	0.29	0.42
Zr	1135	0.26	0.40
La	1138	0.26	0.30
Fe(δ→γ)	1665	0.11	0.06

2.4.2 Defect driven condensation of static displacements

Static displacement towards the product phase but still within the parent phase have been reported in many alloyed systems. Prominent examples are the ω phase alloy $Zr_{0.8}Nb_{0.2}$ [27] and the shape memory alloys $Ni_{1-x}Al_x$ [28] and $Ni_{0.5}Ti_{0.5}$[29]. It was one of the surprises of the neutron measurements in β-Zr and other pure metals that no truly elastic scattering has been observed at these points in reciprocal space where the phonons are overdamped. *From this arises the question to which extent these static precursors of the martensitic transition are defect related or alternatively generic to the transition.*

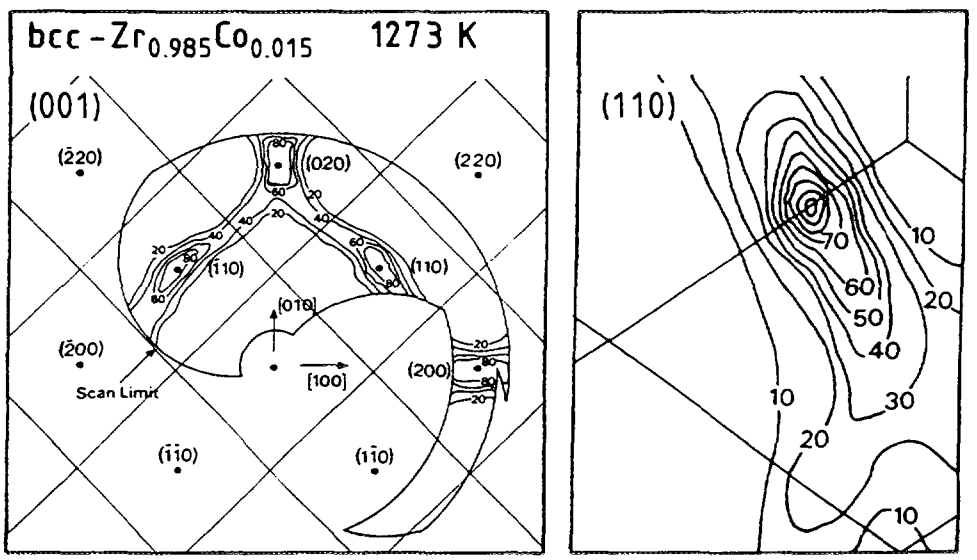

Fig. 14 "Truly" diffuse scattering in bcc-Zr due to alloying of 1.5 at % Co [30].

A first answer is quickly given: A considerable part of what has been reported in literature about elastic precursors related to martensitic transitions is simply due to heterogenous co-existence of product and parent phase. Reasons for this co-existence might be temperature gradients, concentration gradients, impurity driven phase separation, thermal non-equilibrium conditions etc ... A representative example of how gaseous impurities are the driving force for a strongly temperature dependent segregation has been reported for α-precipitates in β-Zr due to oxygen and nitrogen contamination [21].

As stated before diffuse scattering at zero energy transfer in pure samples of the bcc high temperature phase is of inelastic nature. The situation changes upon alloying. With increasing amount of impurities the elastic intensity increases at certain regions in reciprocal space with respect to the neighbouring inelastic intensity. The *difference* between both is then due to *truly elastic* diffuse scattering [11,30]. In reciprocal space this additional elastic diffuse intensity is found exactly along the valley of the low energy and strongly damped phonons. Fig. 14 gives the example of β-Zr alloyed with 1.5 at % Co [30]. Almost similar diffuse patterns are observed for impurities of a so different nature as O, N, Co, or Nb [31]. Only the strength of the effect changes.

In the pure elements the displacements towards the close packed structures are of purely dynamical nature. The existence of diffuse elastic scattering in the presence of point defects indicates that parts of the fluctuations freeze to static displacements. This can be understood in terms of a Kanzaki force analysis. Then, in the limit of low defect concentrations the diffuse scattering cross section can be written [32]:

$$\frac{d\sigma}{d\omega} = c_h c_d \left\langle \left| L(\vec{Q}) + i b_h \vec{Q} \tilde{u}(\vec{q}) + \ldots \right|^2 \right\rangle e^{-2W} \tag{7}$$

c_h, c_d are the host and defect concentrations and b_h, b_d the corresponding coherent scattering lengths. For substitutional defects the Laue term $L(\vec{Q}) = b_d - b_h$ becomes independent of $\vec{Q}$. $\tilde{u}(\vec{q})$ is the Fourier transform of the defect caused displacements in real space $\vec{u}(\vec{r})$. For sufficiently small displacements these are formally ascribed to short ranged Kanzaki forces $\vec{f}(\vec{r}_n)$

$$u_\alpha^m = \sum_{\beta,n} G_{\alpha\beta}^{mn} \cdot f_\beta^n \tag{8}$$

$$G_{\alpha\beta}^{mn} = \int_{1.BZ} D_{\alpha\beta}^{-1}(\vec{q}) \cdot e^{i\vec{q}(\vec{r}_m - \vec{r}_n)} d\vec{q} \tag{9}$$

The dynamical matrix $\overline{\overline{D}}(\vec{q})$ - eq. (2) - which enters into eqs. (8-9) relates the static displacements to the phonon dispersion or lattice potential. As seen in eq. (7) the diffuse elastic scattering is proportional to the scattering vector $\vec{Q}$ times the Fourier transform of the displacement field $\tilde{u}(\vec{q})$. In main symmetry directions such as <111> or <110> the dynamical matrix contains only the square of the longitudinal and transverse phonon energies. Therefore, independently of any model for the displacement field, the diffuse intensity is already proportional to $(\hbar\omega)^{-4}$. *Consequently, diffuse intensity strongly correlates with low energy phonons.* Physically that means that in the presence of defects dynamical fluctuations freeze into static displacements. In the case of β-Zr it could be shown that the displacement field in the presence of defects is a superposition of all the displacements for which low energy phonons are observed [30]. Assignments like diffuse scattering due to ω-embryos are oversimplifications, they arise from measurements of the diffuse scattering only in the [110] plane and oversee its 3-dimensional character.

The absense of elastic precursors is not limited to transitions in monoatomic pure samples. The measurements on a series of Cu based shape memory alloys by Manosa and co-workers [33] confirm the observation that diffuse elastic scattering which might be related to the martensitic transition can be avoided if the alloys are carefully prepared and annealed.

Keeping in mind that at least in the examples cited above diffuse elastic scattering is rather a consequence of defects in the parent phase, than a property inherent to the martensitic transition, a scenario which describes the martensitic transition as a uniform transformation driven by a free energy difference seems to be appropriate. Heterogenous nucleation at defects might play a role for the transition in cases where they are present, however, they are certainly not a necessary prerequisit for the martensitic transformation.

2.4.3 Local symmetry breaking

It is evident from Figs 5 and 13 that the transverse phonons along [ξξ2ξ] and [ξξ0] are strongly damped. Close to or at the BZ boundary the lifetime of the excitations are only of the order of a few vibrational periods. Phonon-phonon interactions can be seen as the physical origin behind these short lifetimes. In a first approximation one-phonon events decay into two one or more phonons, and vice versa multi-phonon events combine to one phonon. Interference effects due to this multi-phonon creation and annihilation have been observed and discussed initially for the quantum solid ^{4}He. In a theory reviewd by Glyde [34] alterations of the one-phonon scattering law $S(Q,\omega)_{1\ phonon}$ are expressed in terms of the observed damping $\Gamma(\vec{q})$

$$S(\vec{Q},\omega)_{interf.} = S(\vec{Q},\omega)_{1phonon}\left\{1 + A(\vec{Q},\vec{q}) + B(\vec{Q},\vec{q},\omega,\omega_0(\vec{q}),\Gamma(\vec{q}))\right\} \quad (10)$$

A first contribution A alters the one-phonon scattering law for apparently equivalent loci in reciprocal space, and a further contribution B affects the one-phonon line shape itself. These latter alterations are explicitely expressed in terms of the damping $\Gamma(\vec{q})$.

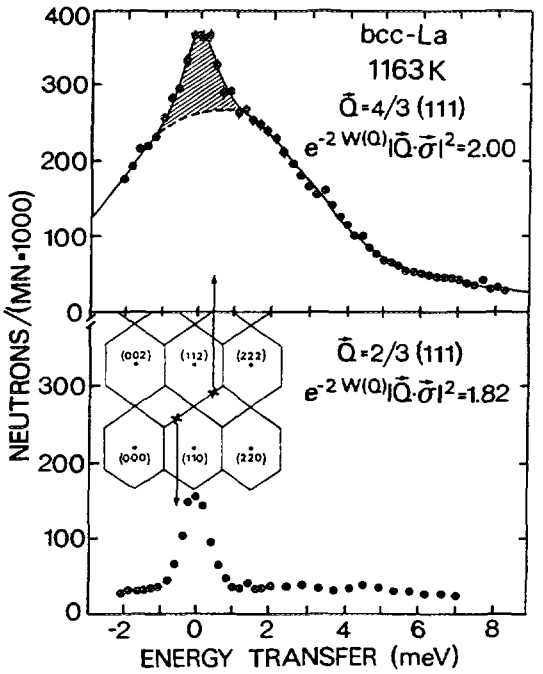

Fig. 15: The L2/3(111) phonon measured in γ-La at two different but equivalent loci in reciprocal space. The one-phonon structure factor $f(\vec{Q})$ for the two points differs by only 10 % [14].

Fig. 15 gives strong evidence for this apparent breaking of cubic symmetry. Measurements of the L2/3(111) phonon in γ-La at different but equivalent $\bar{q}$-values result in a completely different dynamical response. By no means can this be explained by the $\bar{Q}$-dependent structure factor of the one-phonon scattering law $f(\bar{Q})$, which varies for the actual case by 10%. We will not go into detail concerning a quantitative analysis rather present the physical picture which emerges. Because L2/3(111) phonon intensities and line shapes are so different at equivalent points in reciprocal space, we have to conclude that the displacements due to the L2/3(111) phonon locally break the bcc symmetry. (111) planes fluctuate towards the ω structure, however during the second half of the wave period amplitudes are so damped that displacements towards the anti-ω structure are strongly suppressed [14,35].

2.4.4 Anomalous diffusion

At half the melting temperature T_m self diffusities $D(T)$ in the elementary bcc structures vary by roughly 8 orders of magnitude [36]. Elements with martensitic transitions show the highest diffusivity rate whereas the most stable bcc metals of group 6, Cr, Mo, and W have particularly low diffusivities. Direct [37] and indirect measurements [36] of the diffusion mechanism lead to the conclusion that despite the great variety in D, one and the same mechanism is responsible for the self diffusion in all bcc metals, namely the diffusion via nearest neighbour vacancies. *The question, why $D(1/2T_m)$ differs so much, if the same mechanism is valid, remains.* Of course it is appealing to suspect a relation between the tendency of the bcc metals to undergo phase transitions and their unusual diffusivities. In Fig. 16 the possible connection is shown: The L2/3(111) as well as the $T_1$1/2(110) phonon displace the lattice in such a way that atoms are pushed into the direction of an eventually present nearest neighbour vacancy. As argued before, these displacements are of large amplitude in those metals which exhibit "weak" bcc structures, i.e. the phonons tell us that migration barriers are extraordinarily low. Of course diffusion is not only promoted by the two phonons shown in Fig. 16 but by the whole set of displacements related to the tendency of the bcc metals to undergo transitions.

This idea has been worked out more quantitatively [38] and the migration barrier H^m could be expressed in terms of a purely structural term $\alpha \cdot a^2$ characteristic for *all bcc* phases and a term explicitely reflecting the dynamical response of the actual lattice

$$H^m = \alpha \cdot a^2 \left(\int \frac{Z(\omega)}{M\omega^2} d\omega \right)^{-1} \qquad (11)$$

Here a is the lattice constant, M the atomic mass, and the weighting of the phonon density of states $Z(\omega)$ by ω^{-2} guarantees the dominating influence of the low energy phonons.

This model which relates the diffusion anomalies in bcc metals to varying migration barriers has been very successful in explaining the different experimental facts: i) The calculated H^m is close to the measured values, ii) the pronounced chemical group systematics observed in the diffusivity and H^m is reproduced and iii) migration barriers

are established as temperature dependent quantities, with gradients in opposite directions for bcc metals as different as β-Zr and Cr. Fig.17 compares calculated and measured H^m and also indicates the lattice dynamical reason for the systematic variation of H^m .

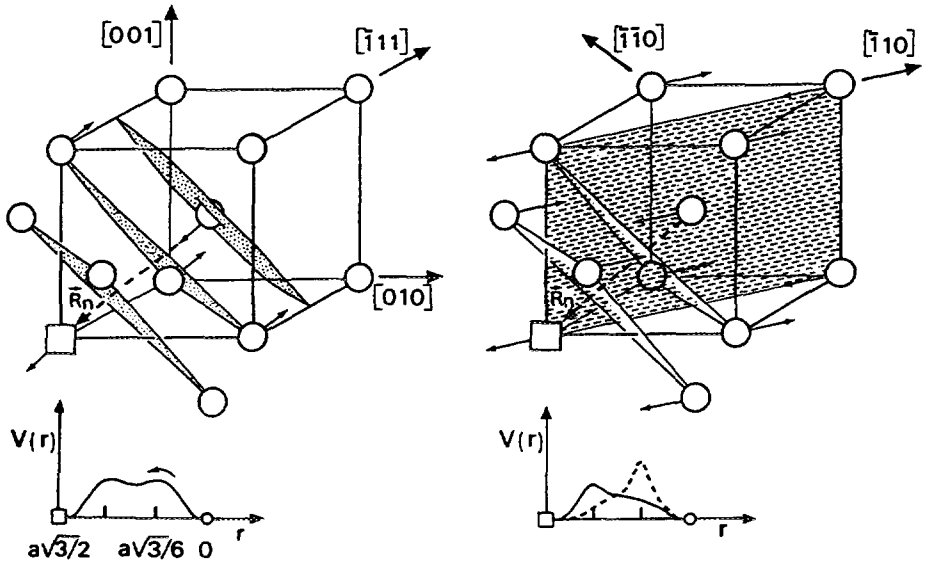

Fig. 16: The displacements of the L2/3(111) (left) and the $T_1$1/2(110) phonon (right) push the centered atom in direction of an eventually present nearest neighbour vacancy. At the left a quasi-static double peak potential is seen by the migrating atom. At the right the phonon itself alters the barriers which it has to overcome during a vibrational period [36].

3 TRANSITIONS FROM CLOSE PACKED STRUCTURES → BCC

The most straight forward examples are the transitions of the low temperature α or hcp phases of the group 4 metals Ti, Zr or Hf to high temperature bcc. No dynamical precursors have been found so far, which is in itself not astonishing. As known from ground state calculations [39] hcp is the structure with the lowest internal energy and as argued before bcc is mainly stabilized by vibrational entropy of the bcc phase itself.

A more promising example could be the invar system Fe_3Pt. Here a strong composition and ordering dependent martensitic transition from a high temperature fcc phase to a low temperature bcc phase is found [40]. According to the Nishiyama-Wassermann rule

$$(111)\text{fcc} \,||\, (110)\text{bcc} \text{ and } [1\bar{1}0]\text{fcc} \,||\, [001]\text{bcc}$$

$(111)[11\bar{2}]$ shuffles are needed to transform the fcc ABCABC... stacking sequence to a ABAB... stacking sequence of $(110)_{bcc}$ planes. Despite several precise neutron and ultrasonic measurements particularly along the $T_{[11\bar{2}]}[\xi\xi\xi]$ branch no anomalies evidently connected to the transition could be identified [41,42]. Instead a pronounced decrease of the $T_{[1\bar{1}0]}$1/2(110) phonon similar to that observed in the bcc metals was found in the austenitic fcc phase [41]. Whether the displacements of this phonon are related to the transition remains to be solved.

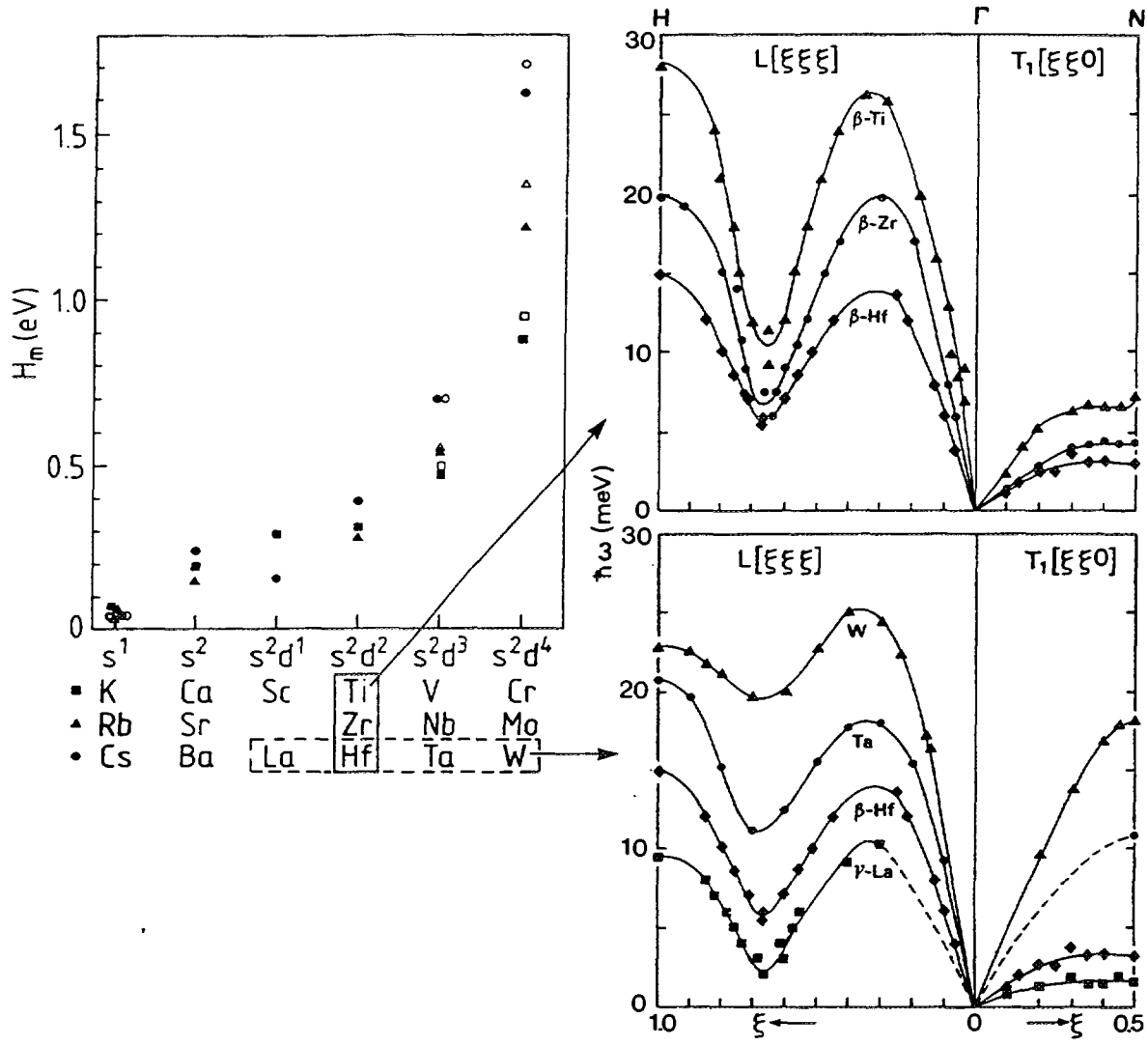

Fig. 17: Left: Migration barriers H^m calculated (black sympols) according to the model of phonon controlled diffusion and compared to measured values (open symbols). Right: Explanation of the chemical group systematics by low energy phonons [38].

4 THE FCC → HCP TRANSITION

Co is an often discussed example. At $T_0 = 695$ K the high temperature phase of fcc-Co transforms to the low temperature hcp structure. For the transition closest packed stacking sequences have to change from ABCABC... to ABAB... Several models have been proposed for the transition, for instance Shapiro and Moss [43] postulate the coherent superposition of two $(111)[11\bar{2}]_{fcc}$ shuffles with wavelength of $\lambda_1=3d_{111}$ and $\lambda_2=6d_{111}$, and more recently Folkins and Walker [44] showed a transition path which is the sum of a modulation and a strain. However, experiments so far are at variance to all these explanations. Firstly, most of the experiments were done on alloyed crystals [43] and secondly, recent careful measurements along $T_{[11\bar{2}]}[\xi\xi\xi]_{fcc}$ in pure Co in the fcc as well as in the hcp phase [45] did not reveal any dynamical anomaly related to the transition. The only experimental hint that Co indeed transforms by shearing $(111)_{fcc}$ planes comes from relatively low energies of the T[ξξξ] phonon branch at short as well as long wavelengths.

A very pronounced phonon anomaly, has been found in fcc or β-La which transforms upon cooling at 609 K to d-hcp. At $\xi = 0.42$ the dispersion along T[ξξξ] branch exhibits a strong temperature dependent dip [46]. However, this example might not be conclusive. The anomaly is only present in metastable β-La below room temperature.

5 SUMMARY

From phonon measurements, shuffles have been identified which promote the transition from bcc towards ω, hcp or fcc. With the exception of the bcc → ω transition the shuffles alone cannot transform the lattice, further homogenous strains are needed. In none of the cited examples do elastic precursors or defects play any obvious role during the transition, which favours the picture of a free energy driven uniform transformation of the entire crystal. The phonon dispersions in the transition elements of group 3 and 4 indicates low restoring forces for fluctuations not only towards one discrete close packed structure but to all of them. The one which locks in at the transition cannot be judged from the phonons alone but is rather a question of subtle details of the internal energy.

The tendency of the bcc metals to transform has severe consequences on the physical properties of these metals. Vibrations in these crystals behave liquid-like along certain directions in reciprocal space. The inelastic response breaks cubic symmetry and can only be explained by phonon-phonon interaction. These dynamical fluctuations promote both the stability of bcc by entropy and the transformation because they are indicative for low restoring forces. Further, self diffusion in bcc can be explained by low migration barriers, the height of which is given by the low energy phonons probing the harmonic part of the migration potential.

The situation is much less clear for the reverse transition, namely close packed → bcc. No shuffle can be identified, only low shear constants are observed. The situation is similar for the transition within closest packing. Further experiments on better defined, if possible, elementary systems and at transitions at high temperature are necessary. Whereas high temperature certainly hinders the experimental access, it is the best way to guarantee the oberservation of the martensitic transitions in thermal equilibrium and due to the higher thermal energy, pinning of the transition on defects is less probable.

6 REFERENCES

[1] Young D.A., Phase diagrams of the elements (University of California Press, Berkeley, 1991)

[2] Delaey L., in Phase Transformations, Material Sience and Technology Vol.5, Vol ed. P. Haasen (VCM Weinheim 1991) pp.339

[3] Petry W., Flottmann T., Heiming A., Trampenau J., Alba M. and Vogl G., *Phys. Rev. Lett.* **61** (1988) 722

[4] Schwarz W., Blaschko O. and Gorgas I., *Phys. Rev. B* **44** (1991) 6785; Smith H.G., Berliner R., Jorgensen J.D., Nielsen M. and Trivisonno J., *Phys. Rev. B* **41** (1990) 1231

[5] Schwarz W., Blaschko O. and Gorgas I., *Phys Rev. B* **46** (1992) 14448; Smith H.G., Berliner R., Jorgensen J.D and Trivisonno J., *Phys. Rev. B* **43** (1991) 4524; Blaschko O. and Krexner G., *Phys. Rev. B* **30** (1984) 1667

[6] Ye Y.Y., Chan C.T., Ho K.-M. and Harmon B.N., *Int.J. Supercomput. Appl.***4**, (1991) 111

[7] Gooding R.J. and Krumhansl J.A., *Phys. Rev. B* **38** (1988) 1695; Gooding R.J., Ye Y.Y., Chan C.T., ho K.-M. and Harmon B.N., *Phys. Rev. B* **43** (1991) 13626
[8] Stassis C., Zarestky J., Wakabayachi N., *Phys. Rev. Lett.* **41** (1978) 1726; Stassis C.and Zarestky J., *Solid State Comm.* **52** (1984) 9
[9] Flottmann Th., Petry W., Serve R. and Vogl G., *Nucl. Instr. & Methods A* **260**, (1987) 165
[10] Petry W., Heiming A., Trampenau J., Alba M., Schober H.R. and Vogl G., *Phys. Rev. B* **43** (1991) 10933
[11] Heiming A., Petry W., Trampenau J., Alba M., Herzig C., Schober H.R. and Vogl G., *Phys. Rev. B* **43** (1991) 10948
[12] Trampenau J., Heiming A., Petry W., Alba M., Herzig C., Miekeley W.and Schober H.R, *Phys. Rev. B* **43** (1991) 10963
[13] Petry W., Trampenau J., Herzig C., *Phys. Rev. B* **48** (1993) 881
[14] Güthoff F., Petry W., Stassis C., Heiming A., Hennion B., Herzig C.and Trampenau J., *Phys. Rev. B* **47** (1993) 2563
[15] Ho K.-M., Fu C.-L. and Harmon B.N., *Phys. Rev B* **28** (1983) 6687; *Phys. Rev B* **29** (1984) 1575
[16] Shaw W.M., Muhlestein L.D., *Phys. Rev B* **4** (1971) 969
[17] Trampenau J., Petry W., Herzig Ch., *Phys. Rev B* **47** (1993) 3132
[18] Burgers W.G., *Physica* **1** (1934) 561
[19] Lingard P.-A. and Mouritsen O.G., *Phys. Rev. Lett.* **57** (1986) 2458
[20] Krumhansl J.A. and Gooding R.J., *Phys. Rev. B* **39** (1989) 3047
[21] Heiming A., Petry W., Trampenau J., Alba M., Herzig C. and Vogl G., *Phys. Rev. B* **40** (1989) 11425
[22] Chen Y., Ho K.-M. and Harmon B.N., *Phys. Rev. B* **37** (1988) 283
[23] Guenin G., Rios Jara D., Morin M., Delaey L., Pynn R. and Gobin P.F., *J. Physique (Paris), Colloque* **43** (1982) C4-597
[24] Neuhaus J., Nicolaus K., Petry W, Hennion B., Krimmel A., to be published
[25] Schober H.R. and Petry W. in Structure of Solids, Material Science and Technology, Vol 1, Vol. ed. V. Gerold (VCH-Weinheim 1993) pp.289
[26] Planes A., Manosa L., Rios-Jara D. and Ortin J., *Phys. Rev. B* **45** (1992) 7633; Manosa L., Planes A., Ortin J. and Martinez B., *Phys. Rev. B* **48** (1993) 3611
[27] Noda Y., Yamada Y. and Shapiro S.M., *Phys. Rev. B* **40** (1989) 5995
[28] Shapiro S.M., Yang B.X., Noda Y., Tanner L.E. and Shryvers D., *Phys. Rev B* **44** (1991) 9301
[29] Müllner M., Tietze H., Eckold G. and Assmus W. in Proc. Int. Conf. Martensitic Transformations, ICOMAT 86, Nara (Japan), ed. I. Tamura (The Japan Inst. of Metals 1987) pp.159
[30] Heiming A., Petry W., Vogl G., Trampenau J., Schober H.R., Chevrier J. and Schärpf O., *Z. Phys. B* **85** (1991) 239
[31] Petry W., *Phase Transitions* **31** (1991) 119
[32] Bauer G.S., in Treatise on materials science and technology ed. by G. Kostorz, Vol 15 (Academic Press, New York 1979) p. 291
[33] Manosa L., Zarestky J., Lograsso T., Delaney D.W. and Stassis C., *Phys. Rev. B* **48** (1993) 15708
[34] Glyde H.R., *Can. J. Phys.* **52** (1974) 2281
[35] Dubos O., Petry W., Trampenau J. and Hennion B., unpublished
[36] Petry W., Heiming A., Herzig C. and Trampenau J., *Defect & Diffusion Forum* **75** (1991) 211

[37] Vogl G., Petry W., Flottmann T. and Heiming A., *Phys. Rev. B* **39** (1989) 5025
[38] Schober H.R., Petry W. and Trampenau J., *J. Phys. Condens. Matter* **4** (1992) 9321
[39] Pettifor D.G.. in Structure of Solids Material Science and Technology, Vol 1, Vol. ed. V. Gerold (VCH-Weinheim 1993) pp.61
[40] Wassermann E.F. in Ferromagnetic Material Vol 5, eds K.H. Buschow, E.P. Wollfarth (North Holland, Amsterdam 1990) pp.240
[41] Noda Y. and Endoh Y., *J. Phys. Soc. Japan* **57** (1988) 4225
[42] Kawald U., Schulenberg P., Bach H., Pelzl J., Eckold G. and Saunders A., *J. Appl. Phys.* **70** (1991) 6537
[43] Shapiro S.M. and Moss S.C., *Phys. Rev. B* **15** (1977) 2726
[44] Folkins I. and Walker M.B.., *Phys. Rev. Lett.* **65** (1990) 127
[45] Strauß B., Frey F., Petry W., Trampenau, J. Nicolaus K.,. Shapiro S.M., Bossy J.,*Phys. Rev. B*, in press
[46] Stassis C., Smith G.S., Harmon B.N., Ho K.-M. and Chen Y., *Phys. Rev. B* **31** (1985) 6298